# THEORETICAL STUDIES OF CATALYSIS BY CARBOXYPEPTIDASE A: COULD GAS-PHASE CALCULATIONS SUPPORT A MECHANISM?

Alexandra KILSHTAIN-VARDI[a1,b], Gil SHOHAM[a2] and Amiram GOLDBLUM[b1,*]

[a] *Department of Inorganic and Analytical Chemistry, Institute of Chemistry, Hebrew University of Jerusalem, Israel 91120; e-mail:* [1] *alexvardi@lycos.com,* [2] *gil2@vms.huji.ac.il*

[b] *Department of Medicinal Chemistry and the David R. Bloom Center for Pharmacy, School of Pharmacy, Hebrew University of Jerusalem, Israel 91120; e-mail:* [1] *amiram@vms.huji.ac.il*

Received September 20, 2002
Accepted April 7, 2003

*Dedicated to Professors Petr Čársky, Ivan Hubač and Miroslav Urban on the occasion of their 60th birthdays.*

We compare recent quantum mechanical computations of alternative reaction pathways for carboxypeptidase A, a zinc proteinase, in an "enzyme environment" to similar calculations in the "gas phase" that include the minimal chemical entities that are required for a non-catalytic reaction. The main question that we address is whether anything may be learned from such reduced representations. Two general acid-general base alternative pathways and one nucleophilic pathway are compared. The original calculations were run on a relatively large model (120 atoms) of the active site of carboxypeptidase A which included zinc and its ligands, as well as the residues Arg145, Arg127, Glu270, a water molecule and a model dipeptide. The "gas-phase" pathways include only the dipeptide, water and Glu270 and serve as models for the non-catalytic pathway. The calculations were performed by semiempirical MNDO/H/d that includes modifications for d-orbital representations as well as for intra- and intermolecular multiple H-bond formation. The gas-phase results strengthen our previous conclusion about the preference for general acid-general base pathways for peptide cleavage by carboxypeptidase A rather than a "direct nucleophilic" pathway. The bottleneck of the reaction is proton transfer to the nitrogen in the peptide bond, preceding the peptide cleavage.

**Keywords**: Carboxypeptidase A; Enzymes; Proteinases; Inhibitors; Catalytic mechanism; MNDO/H; MNDO/d; General acid-general base; Reaction coordinate; Gas phase; Semiempirical calculations; Peptidomimetics.

Zinc metalloproteinases comprise a large family of enzymes with a wide variety of biological roles. These enzymes are characterized by the presence of at least one coordinated zinc ion as an essential catalytic component[1]. Zinc

metalloproteinases such as angiotensin converting enzyme[2] (ACE), enkephalinase[3], collagenase[4] and other matrix metalloproteinases[5] are involved in disease conditions, and their inhibition is expected to block some damaging excessive activity. For ACE, a few "generations" of inhibitors have already been marketed and are major antihypertensive drugs. The first ACE inhibitors were developed on the basis of analogies between ACE and the then known structure of carboxypeptidase A[2] (CPA). Also, inhibitors of ACE were discovered to be good inhibitors of CPA[6]. The primary function of CPA, a digestive enzyme, is to degrade intake proteins[7]. Pancreatic CPA catalyzes the hydrolysis of the terminal residue at the C-terminal of peptide and ester substrates.

Catalytic data and structure studies of these enzymes are necessary for better understanding of their function, and are essential for computerized design of drugs by methods that are generally known as "structure-based drug design". Many structure studies were performed on CPA[8–10] and it is generally accepted that CPA is a good representative of this family, and that the catalytic mechanism of action is common at least to most of the zinc proteinases[11–13].

Despite some differences in folds, in zinc-binding motifs and in active site topologies, all of these enzymes have a single catalytic zinc(II) ion at the active site with a very similar coordination. Three of these coordination sites are occupied by protein ligands and the fourth coordination site is labile, and serves for the binding of water, substrates and inhibitors[14,7].

The three-dimensional structure of native CPA has been determined at a high resolution of 1.5 Å[9,10]. In the active site it has a zinc ion coordinated to three functional groups of side chains (His69, Glu72 and His196) and a water molecule. A nucleophile (Glu270) and an electrophile (Arg127) are close to the zinc ion and to the zinc-bound water. Despite the large amount of data from kinetic studies and from X-ray crystallography for various zinc proteinases, there is no agreement as yet concerning the details of the catalytic mechanism of this family. Generally, two major types of catalytic mechanisms have been proposed for CPA: (i) A direct nucleophilic attack (initially called "Zn-carbonyl mechanism" or "acyl pathway") on the peptide carbonyl by Glu270, resulting in the formation of an anhydride intermediate. (ii) General acid-general base (GAGB) mechanisms ("Zn-hydroxide mechanism" or "promoted water pathway"), in which a water molecule initially attacks the carbonyl while, or after, losing a proton. GAGB results in the formation of a gem-diol intermediate which has, most probably, at least a mono-charged state due to positions of its oxygens near zinc.

In the direct nucleophilic mechanism[12], the incoming substrate initially displaces the zinc-bound water, and the peptide carbonyl interacts directly with the zinc ion and is activated by it. In this "waterless" environment, the negatively charged Glu270 attacks the carbonyl carbon and the amide bond is subsequently cleaved. Following this cleavage, an "acyl enzyme" (acylated Glu270) is formed and is, in this case, an anhydride. In a second step, this anhydride is cleaved by water.

Experimental support for the direct nucleophilic pathway was based on the spectroscopic detection of anhydride-type acyl-enzyme intermediates in the CPA-catalyzed hydrolysis of ester substrates under low-temperature conditions[15–18]. But these findings were challenged[13,17]. Recent solid-state NMR spectroscopy[19] and X-ray studies of a Gly-Tyr complex with CPA [20] support the anhydride path to some extent. Earlier isotopic studies by Breslow and Wernick showed that an anhydride intermediate is probably not involved in the hydrolysis of peptide substrates by CPA, and suggested that this cleavage is better rationalized by a general acid-general base mechanism[21,22]. In GAGB, a water molecule, which is activated by the zinc or by Glu270, attacks the peptide bond, loses a proton (probably to Glu270) and forms a gem-diol intermediate. Low-temperature studies reported by Auld and coworkers[23] supported these suggestions. Moreover, recent kinetic experiments show that it may be possible that different mechanisms operate with different substrate types: peptide hydrolysis could take place *via* a GAGB mechanism, while ester hydrolysis could follow the anhydride mechanism path[24,25].

There are two main proposals for a GAGB pathway of CPA. Christianson and Lipscomb[20] suggested a reaction path in which the substrate binds directly to zinc while retaining the water molecule that occupies the fourth coordination site of zinc in the native structure. In such a mechanism, this water molecule may be activated by the metal ion or by Glu270 (or both), it may lose a proton and attack the peptide carbonyl. This suggestion for a GAGB mechanism was based on crystallographic results of CPA complexes with transition state analogue inhibitors[26,27] that bind to the active site as gem-diols. However, the charge state of such gem-diols, whether neutral or negative, is not known. The two tetrahedral oxygens of the gem-diol moiety are stabilized by their interactions with zinc. The gem-diol moiety by itself is highly unstable in solution, unless strong electron attractors are substituted near the carbonyl[28]. Crystallographic structures of CPA complexes with ketomethylene inhibitors, which were determined in our laboratory[29] reveal a gem-diol intermediate coordinated to zinc through both oxygens. It should be noted that it was experimentally shown that a

gem-diol moiety is formed only as a result of the interaction with the enzyme, while none were detected in solution if no enzyme was present[28].

A significantly different GAGB mechanism was proposed by Mock[30] based on kinetic studies of two diastereoisomers. The binding of the substrate enables activation of the peptide carbonyl by zinc as in the above mechanism, but the relevant water molecule is positioned very differently. Mock proposed that this water molecule is deprotonated by the C-terminal carboxylate of the substrate itself, which is adjacent to Arg127, and not by Glu270 or by the zinc ion. The following steps in this mechanism are analogous to the previously described GAGB, but the directions inside the enzyme and the internal distances from the catalytic groups are different in the "Mock mechanism" compared to the "Lipscomb mechanism".

Several theoretical studies have been performed in order to clarify the catalytic mechanism of the representative zinc metalloproteinases CPA and thermolysin (TLN). Morokuma and coworkers[31] employed *ab initio* STO-3G calculations and demonstrated that in the case of CPA the p$K_a$ of the Zn-coordinated water molecule is lowered due to Zn, and this water acts as a proton donor for Glu270. Alex and Clark[32] found that the concerted addition of the $ZnOH^{+1}$ moiety to the carbonyl bond of a formamide (model substrate) was found to be the rate-determining step of the overall reaction.

Alvarez-Santos *et al.*[33] designed a model in which the attack of the hydroxide ion oxygen on the carbonyl carbon of the scissile peptide was found to be the rate-determining step, with a high enthalpy barrier of 37.9 kcal/mol. This enthalpy barrier was dramatically decreased when a positive charge, representing Arg127, was included. More recent results from that group show that the transition state for proton transfer from Glu270 to the peptide nitrogen is the highest peak in the full energy profile. Abashkin *et al.*[34] performed density-functional theory calculations on CPA, but had to reduce the size of the model to 26 atoms. Their results[34] suggest that the rate-determining step is the formation of a tetrahedral intermediate resulting from the attack of a Zn-coordinated OH group on the carbonyl of the substrate. A semiempirical QM study of the GAGB and anhydride mechanisms of CPA was recently performed by our group, suggesting that proton transfer to the nitrogen of the peptide bond is the rate-determining step of the reaction, which precedes peptide bond cleavage. Our model included 120 atoms and employed the MNDO/d/H method to investigate the alternative reaction coordinate pathways[35].

Molecular dynamics (MD) simulations by Banci *et al.*[36] suggest that both "nucleophilic" and "water-promoted" pathways are structurally feasible, although the water-promoted mechanism is favored energetically. Unfortu-

nately, none of these studies compared the alternatives in a systematic manner, in order to conclude which of them is more likely to represent the mechanism of cleavage by CPA. We have recently compared the two proposed GAGB mechanisms, and concluded that the two GAGB alternatives cannot be easily distinguished: one of the two is preferred on thermodynamic grounds while the other has a somewhat lower activation barrier[35]. In a subsequent paper[37], we showed that the nucleophilic mechanism has a much higher barrier than the two GAGB alternatives, and thus it is not expected to play a role in the enzyme mechanism.

If any of these alternatives is the correct one, it is expected to be a catalytic mechanism, *i.e.*, one which should have a reaction barrier that is higher than its enzyme analogue reaction. In the following we compare the reactions in the enzyme environment to gas-phase computations that were performed in this study by following similar steps to those of the reaction pathways within the enzyme models. The specific question that we address is whether it is possible to obtain support from such gas-phase calculations for determining which of the alternatives should be preferred.

## METHODS

Many decisions had to be taken in view of the relative complexity of the active site of CPA and the need to be as relevant as possible to the various experimental results available. First, we have chosen to initiate this study with our own results for the structure of a crystallographic complex between CPA and the inhibitor pGluFF (Glp-Phe-Ψ($CH_2$CO)-Phe-OH, $K_i$ = $4.7 \times 10^{-7}$ mol/l)[38] as a representative of the ketomethylene inhibitors[39] (see Fig. 1). In this family of inhibitors, the peptide bond is replaced with a carbonylmethylene unit, *i.e.*, the peptide NH group is substituted by a $CH_2$ group. This replacement is sufficient to prevent the cleavage of this substrate analogue due to relative strength of the $CH_2$–CO bond vis-a-vis the peptide bond[40]. For a modeling study, this enables an *in silico* transforma-

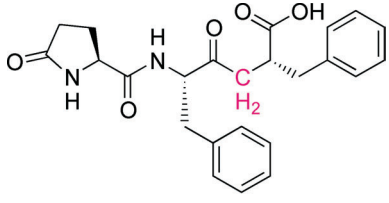


FIG. 1
pGluFF – the ketomethylene inhibitor used as a model for the substrate. The methylene group (in red) may be replaced by NH to form a model of the substrate

tion from an inhibitor to a real substrate by "computerized mutation" of only a single "heavy" atom. With this in mind, our group determined the structure of the CPA/pGluFF complex at high (1.46 Å) resolution and with an excellent crystallographic *R* factor of 13% [39], providing a reliable starting model for the CPA computational studies.

For studying the alternative reaction pathways in CPA, protons were added to the crystallographic structure of CPA/pGluFF using the program pkwater[41] at pH 7.5. The model of the active site included 120 atoms, consisting of the inhibitor (two phenylalanine residues were mutated to alanines and the pGlu ring was transformed to a methyl), zinc, and models for only the most crucial protein residues: Arg127, Arg145, Glu270, His69, His72, His196 – each representing the corresponding side chain starting from its $C_\beta$ atom. Only Glu270 was represented by a longer side chain starting from its $C_\alpha$ atom. The substrate was generated from the inhibitor by a "computerized transformation" of the $-CH_2$ group (adjacent to the carbonyl of the peptide substrate) into an NH group. In the crystal structure of the CPA complex with pGluFF, the ketomethylene moiety is found to be in the gem-diol form, thus incorporating a water molecule (that was bound to zinc in the native structure) as part of the gem-diol. It is however not clear which of the two gem-diol oxygens originated in the ketomethylene and which is the original water oxygen. The enzyme model is depicted in Fig. 2, where 2a presents a scheme of the model while 2b presents the geometry of the residues that were used for modeling the enzyme reaction pathways.

The full model is positively charged ($q$ = +1), due to the presence of zinc (+2) and two arginines (127, 145), each with a charge of $q$ = +1, while negative charges reside on the C-terminal of the inhibitor, on Glu270, and on Glu72 in the coordination sphere of the catalytic zinc. The alternatives for the initial protonation state of the complex with the inhibitor and with the "mutated" substrate were studied by optimizing the geometry of all protons in each of a few alternatives[35] for the configurations of polar protons in the system. This study was first performed with a very large representation of atoms from the active site of CPA (≈500 atoms) and the stability of the results was compared to the smaller model of 120 atoms and found to be satisfactory.

MNDO has been previously demonstrated by Geissner and Jacob[42] to be useful for structures containing zinc complexes, by introducing a proper parametrization for a coordinated zinc ion. Following the development of MNDO/d by Thiel and Voityuk[43], it has been recently demonstrated that this approach has advantages over PM3 or AM1 parametrizations for zinc, at least for structure studies, although it was less successful for reaction

pathways[44]. We have modified, some time ago, the original H-bonding correction to MNDO [45] in order to enable studies of multiple H-bonding systems with both inter- and intramolecular H-bonds[46]. Our modification was later extended to enable proton transfers[55]. Thus, using MNDO/d/H with our own version of multiple H-bonding, implemented into UNICHEM 5.0 [47], includes the advantages of both d-orbitals as well as detecting all types of H-bonding interactions simultaneously. The reaction coordinate method[48] was employed to follow the three alternative pathways. Reaction coordinate variations were performed initially in steps of *ca* 0.01 Å followed by smaller steps around the transition state structures. There was, however,

a

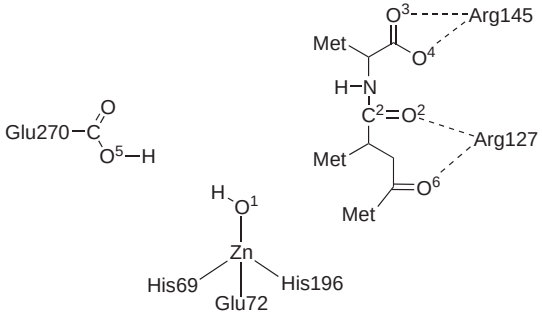


b

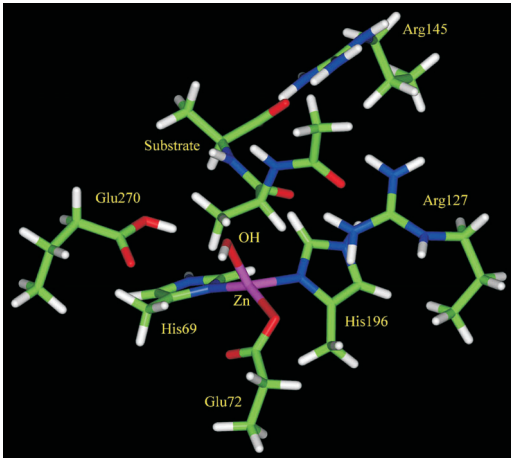


FIG. 2

The model structure for the reaction pathways of this paper. a Scheme of the residues in the enzyme environment model (Met is methyl). b The three-dimensional positions in the enzyme environment model. Zinc, its three ligands and the two arginines were not included in the "gas-phase" study of this paper

no attempt to locate the exact transition state positions through the Hessian matrix eigenvalues, since most of the structure was "frozen" in the optimizations in order not to distort the original crystal structure by allowing unrealistic "drifts" in the positions of the amino acid involved. Only the atoms of the side chains were allowed to optimize along the reaction coordinates. Any attempt to calculate vibrational modes in "restricted" structures should lead to incorrect frequency eigenvalues.

For some proton transfers, the best path was searched by a two-dimensional (2D) reaction coordinate. For example, for proton transfers to the peptide nitrogen it was necessary to extend the peptide bond and to change the H–N distance over a grid. The reaction surface that was produced, $E = E(r_1,r_2)$ was employed for searching the lowest energy path.

For the "gas-phase" reactions in the present study, we employed a minimal representation of the "non-catalyzed" reaction with only the direct participants of the different pathways: the same peptide as in the enzyme reactions, water (which is required for the initial step in GAGB pathways and for the second step in the direct nucleophilic mechanism) and Glu270 (required for the direct nucleophilic pathway). Thus, all three model reactions included the same substrate, water and Glu and may be compared

In the gas-phase model pathways, catalysis does not exist and thus the use of the catalytic terminology of GAGB should have been eliminated. However, for the sake of easy comparison to previous results, we retain the use of GAGB even though these model reactions do not include the catalytic components.

## RESULTS

### *The Gas-Phase Analog of GAGB-1*

The various species along the gas-phase attack of a water molecule on the carbonyl from the direction of Glu270 (GAGB-1) are shown in Fig. 3 and the enthalpy profile for this path is shown in Fig. 4, compared with the energy profile for the enzyme environment. Some features of bond lengths, angles and dihedrals are presented in Table I for species that are presented in Fig. 3, and are compared with features of similar species in the enzyme environment.

Minimization was applied (including all hydrogens, most of each side chain and the full substrate) at each step of the reaction coordinate. To retain the character of the X-ray results for the gem-diol inhibitor, reaction steps started from the intermediate product (INT-1, Fig. 3c), which is the

TABLE I
Geometry variations in the structure of intermediates (INT) and transitions states (TS) for the GAGB pathways of peptide cleavage

| Pathway | Reactants | | | TS-1 | | | INT-1 | | | TS-2 | | | Products | | |
|---|---|---|---|---|---|---|---|---|---|---|---|---|---|---|---|
| | Pb[a] length | Pb[b] dihedral | $C_2$–$O_1$[c] | Pb[a] length | Pb[b] dihedral | $C_2$–$O_1$[c] | Pb[a] length | Pb[b] dihedral | $C_2$–$O_1$[c] | Pb[a] length | Pb[b] dihedral | $C_2$–$O_1$[c] | Pb[a] length | Pb[b] dihedral | $C_2$–$O_1$[c] |
| GAGB-1 enzyme | 1.39 | –164.6 | 2.49 | 1.43 | 166.3 | 1.96 | 1.55 | 100.2 | 1.42 | 1.55 | 92.1 | 1.40 | 4.73 | NA | 1.29 |
| GAGB-1 gas phase | 1.42 | 166.9 | 7.00 | 1.44 | –176.6 | 2.13 | 1.50 | –151.3 | 1.47 | 1.80 | NA | 1.46 | 5.77 | NA | 1.32 |
| GAGB-2 enzyme | 1.50 | –55.8 | 1.51 | 1.50 | –52.6 | 1.51 | 1.51 | –66.9 | 1.51 | 1.63 | –43.5 | 1.39 | 1.85 | NA | 1.35 |
| GAGB-2 gas phase | 1.37 | –161.4 | 5.74 | 1.49 | 58.5 | 1.70 | 1.55 | 41.5 | 1.43 | 1.70 | 41.1 | 1.39 | 5.03 | NA | 1.35 |

[a] Peptide bond length (in Å). [b] Peptide bond dihedral angle (in °). [c] Distance (in Å).

gem-diol of the substrate, back to separated hydroxide ion and carbonyl (Fig. 3a) through the transition state TS-1 (Fig. 3b). Along the breaking of this oxygen–carbon bond, the re-formation of a peptide bond in the substrate was monitored, as well as the ability of the incipient hydroxide ion to "absorb" a proton from the protonated Glu270. In this initial (INT-1) configuration[35], the gem-diol oxygen that is closer to Glu270 is protonated while the other oxygen atom is negatively charged. In the enzyme, the protonation of Glu270 is due to the transfer of a proton from the zinc-bound water molecule. For direct comparison, this state was retained in the absence of zinc.

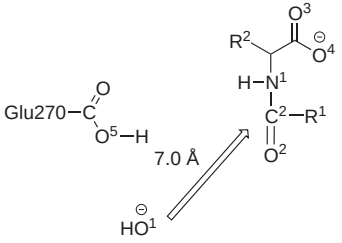


a) Table I, Reactants
Energy = –337.0 kcal/mol

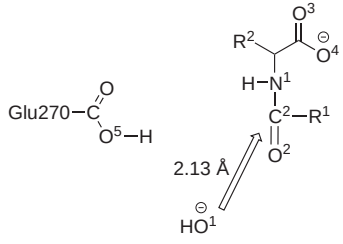


b) Table I, TS-1
Energy = –301.0 kcal/mol

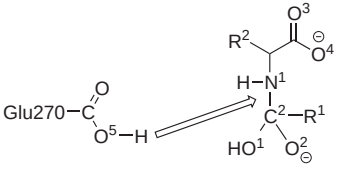


c) Table I, INT-1
Energy = –321.1 kcal/mol

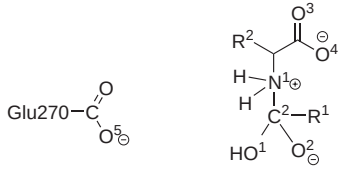


d) Table I, TS-2
Energy = –285.8 kcal/mol

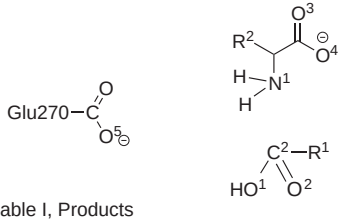


e) Table I, Products
Energy = –341.4 kcal/mol

FIG. 3
Schemes of prevailing structures along the gas-phase "GAGB-1" pathway

For separating the intermediate back to reactants, the hydroxyl–carbonyl bond length was extended from 1.47 Å (in INT-1) in steps of 0.01 Å and minimized at a distance in which the energy changed only slightly. That minimization extended the optimal distance to ≈7.0 Å. In the reactants (Fig. 3a), the distance between the hydroxide ion and the carbon of the carbonyl bond is thus 7.0 Å and the energy is –337.0 kcal/mol. Such a very long distance is attainable in a gas-phase reaction, where other atoms do not interfere in the path as they would if the path had been stretched to such a distance inside the enzyme. The dihedral angle of the peptide bond is 166.9° and its length is 1.42 Å. Starting from the reactants, as the hydroxide ion moves toward the peptide bond, the energy increases up to the transition state (TS-1), in which the distance between the hydroxide ion and the carbon of the carbonyl bond is 2.13 Å and the energy is –301.0 kcal/mol. The peptide bond has now extended just a little, to 1.44 Å. From this point the energy decreases and a gem-diol is formed, its energy being stabilized at –321.1 kcal/mol. The energy barrier for this part of the reaction coordinate is thus 36.0 kcal/mol.

In the next step, the proton transfer reaction, we moved the $O_5$-proton from Glu270 toward the NH of the peptide bond. This experiment started again from the X-ray based structure of the model substrate, INT-1. A 2-dimensional reaction coordinate was constructed as described in Methods. The peptide bond was extended from 1.50 to 1.95 Å in steps of 0.1 Å, while the proton distance from the peptide nitrogen was extended from 1.01 to 2.31 Å in steps of 0.01 Å. The energy barrier for this proton transfer is 35.3

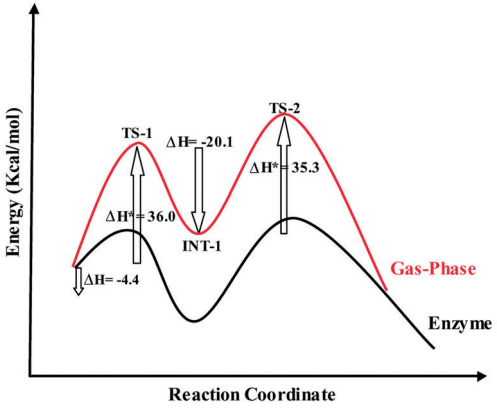


FIG. 4
The enthalpy diagram for the gas-phase (in red) "GAGB-1" pathway compared to the same reaction in the enzyme environment (in black)

kcal/mol (from INT-1 with –321.1 kcal/mol to TS-2 with –285.8 kcal/mol, with the peptide bond fixed at 1.80 Å). Spontaneous extension of the peptide subsequent to proton transfer proceeds with no energy barrier and releases *ca* 55.6 kcal/mol.

*The Gas-Phase Analog of GAGB-2*

This second suggestion for a GAGB mechanism[35] has been studied by following an analogous reaction pathway to that in the enzyme environment. Starting again from a gem-diol intermediate, a water molecule was formed by attaching the proton to the hydroxyl of the gem-diol and "moving back" to a stable starting point. The details of this pathway are presented Fig. 5 (for various species along the reaction) and Fig. 6 (for enthalpy variations along this path and its comparison to the same path in the "enzyme

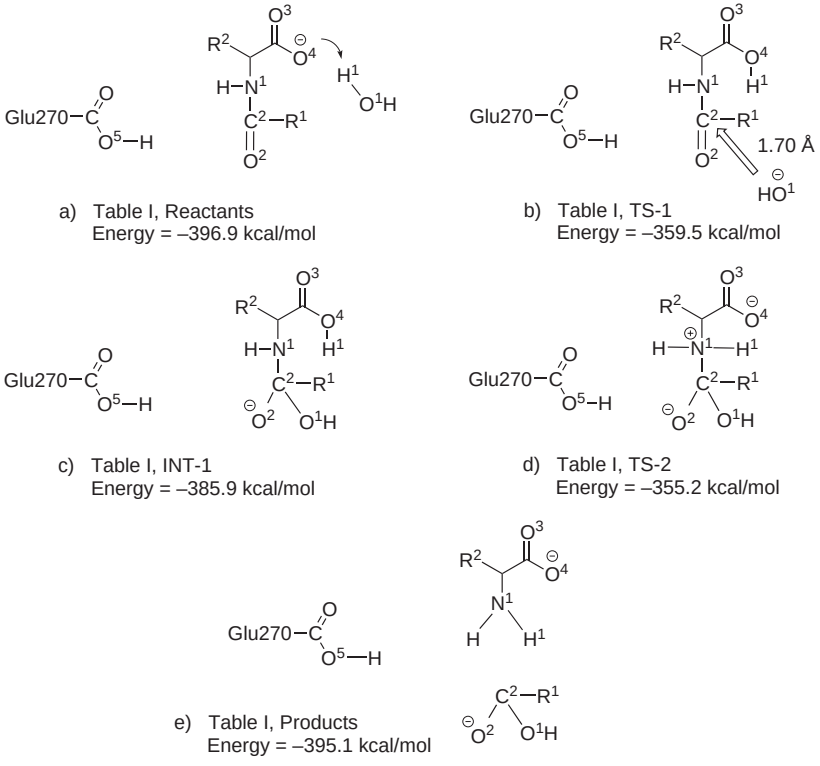


FIG. 5
Schemes of prevailing structures along the gas-phase "GAGB-2" pathway

environment"). Also, similar to the reaction in the enzyme environment, this model requires an additional proton in the system due to convergence problems caused by the proximity of negative charges on Glu270 and on $O_2$ of the gem-diol (originally, $O_2$ is the carbonyl oxygen).

The reaction path started again by extending the $C_2$–$O_1$ distance from INT-1 (Fig. 5c) to a separated hydroxide ion and peptide substrate (Fig. 5a). At a close distance (≈3.0 Å) between the hydroxide oxygen and $O_4$ of the peptide carboxy terminal, the proton at the terminal could be transferred to the hydroxide to form a water molecule with a very low barrier of some 3 kcal/mol. Minimization of the position of the water molecule was finally achieved at a $C_2$–$O_1$ distance of 5.74 Å and at a $O_4$–$O_1$ distance of ≈3.2 Å (Fig. 5a). A 2D-reaction coordinate study was initiated from this point (reactants) with two distances being varied for water, that of the hydroxide ion from the carbonyl of the substrate ($C_2$–$O_1$), and the distance of the proton ($H_1$–$O_1$) from the water fragment, as it was moving toward $O_4$ at the C-terminal of the substrate. The $C_2$–$O_1$ (water) distance was varied from 5.70 to 1.51 Å by steps of 0.01 Å and the $HO_1$–$H_1$ distance was extended from 1.01 to 1.50 Å by steps of 0.01 Å. Proton transfer occurs at a $C_2$–$O_1$ distance of 2.90 Å with a barrier of some 25 kcal/mol. At any other $C_2$–$O_1$ distance this barrier is much higher. Energy is reduced by only some 3 kcal/mol with respect to this barrier, for the fully transferred proton (to $O_4$). The reaction path continues through a barrier of 37.4 kcal/mol at a $C_2$–$O_1$ distance of 1.70 Å (Fig. 5b). Following this barrier, the gem-diol is formed (INT-1). Subsequently, peptide cleavage occurs as a result of proton

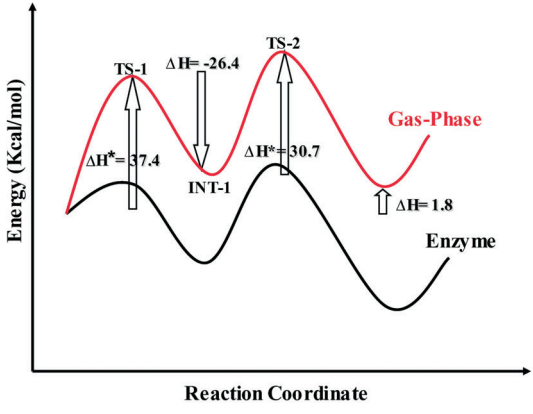


FIG. 6

The enthalpy diagram for the gas-phase (in red) "GAGB-2" pathway compared to the same reaction in an enzyme environment (in black)

transfer to the peptide nitrogen which is more basic in the gem-diol intermediate than in the peptide. Proton transfer from Glu270 to the peptide nitrogen failed again due to convergence problems: such a reaction coordinate creates a negative charge on $O_5$ of Glu270 which is close to the negative charge of the gem-diol. The other proton transfer was more successful. The proton transfer from $O_4$ at the C-terminal of the substrate was done in steps of 0.01 Å. For this proton transfer there is a substantial increase in energy of some 30.7 kcal/mol (from –385.9 kcal/mol to TS-2 with –355.2 kcal/mol, Fig. 5d). At this stage we find that the peptide bond length extends to 1.70 Å, while the proton distance from the nitrogen at the peak of TS-2 is 1.01 Å. Continuing after the TS, the peptide is spontaneously cleaved into products with a final energy of –395.1 kcal/mol.

*The Gas-Phase Analog of the Direct Nucleophilic ("Anhydride") Pathway*

The anhydride pathway was followed by including only Glu270, water and the substrate.

Fig. 7 depicts the various distinct species that were characterized along the reaction pathway for anhydride formation, while Fig. 8 displays the enthalpy diagram for the full pathway compared to the same pathway in the enzyme environment.

The investigation of reaction coordinate started from the structure INT-1 (Fig. 7c) in which Glu270 has already attacked the substrate and a bond has been formed between the oxygen of Glu270 and the peptide carbonyl carbon. The anhydride bond was formed by connecting between the oxygen of Glu270 and the carbonyl carbon of peptide bond in our initial model from X-rays, while the backbone (the $C_\alpha$ of Glu 270) was fixed. During energy minimization of the structure, the substrate was allowed to move freely. From this tetrahedral intermediate, we followed the "backward" reaction, to separated intact peptide and Glu270 (with fixed backbone). Along the breaking of this O–C bond, the re-forming of a peptide bond in the substrate was monitored.

In the GAGB mechanisms, a proton may be donated by Glu270 (as in GAGB-1) or by the peptide terminal carboxylate (as in GAGB-2). In the direct nucleophilic mechanism, water is the only reasonable source for protonation of the nitrogen toward peptide cleavage. The $H_1$ proton was thus moved in steps from the water oxygen to the nitrogen of the peptide.

The reaction coordinate study started from the structure INT-1 (Fig. 7c) in which Glu270 has already attacked the substrate and a bond has been formed between the oxygen of Glu270 and the peptide carbonyl carbon.

From this tetrahedral intermediate, we followed the "backward" reaction, to separated intact peptide and Glu270 along the breaking of this $O_5$–C bond. The "anhydride type" $O_5$–$C_2$ bond length was extended from 1.44 to 2.80 Å in steps of 0.01 Å.

In the initial structure (Fig. 7a, reactants), the distance between the oxygen of Glu270 and the carbon of the carbonyl bond is 2.80 Å and the energy is –346.9 kcal/mol. The dihedral angle of the peptide bond is 171.9° and its length is 1.38 Å. As a bond is formed between Glu270 and the sub-

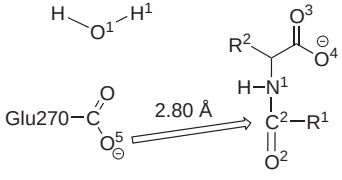


a) Reactants
Energy = –346.9 kcal/mol

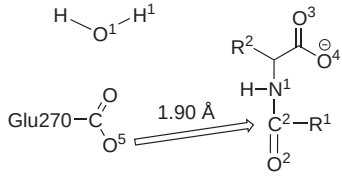


b) TS-1
Energy = –304.0 kcal/mol

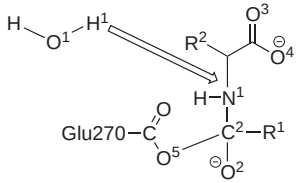


c) INT-1
Energy = –311.2 kcal/mol

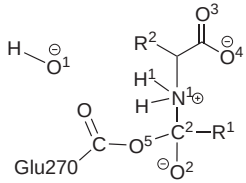


d) TS-2
Energy = –278.8 kcal/mol

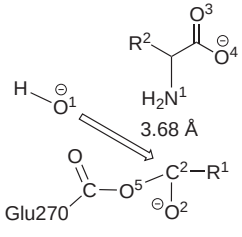


e) INT-2
Energy = –298.8 kcal/mol

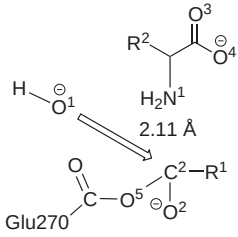


f) Table 1, TS-3
Energy = –286.3 kcal/mol

FIG. 7
Schemes of prevailing structures along the gas-phase nucleophilic mechanism

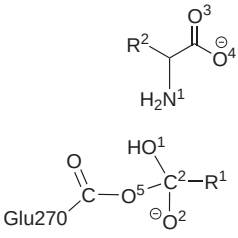


g) INT-3
Energy = –316.6 kcal/mol

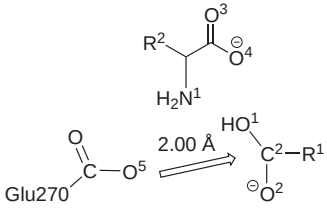


h) TS-4
Energy = –310.2 kcal/mol

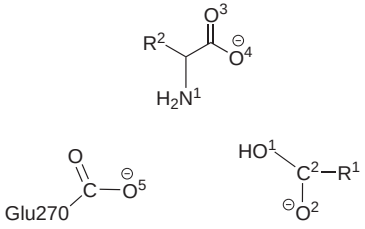


i) Products
Energy = –359.3 kcal/mol

FIG. 7
(*Continued*)

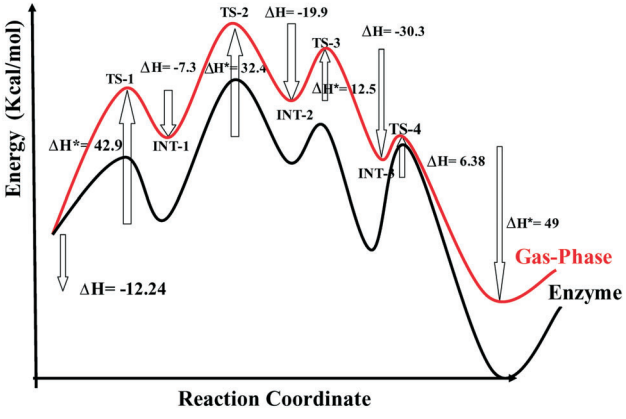


FIG. 8
The enthalpy diagram for the gas-phase (in red) nucleophilic ("anhydride") pathway compared to the same reaction in an enzyme environment (in black)

strate, the energy increases until it reaches TS-1, in which the distance between the oxygen of Glu270 and the carbonyl carbon is 1.90 Å and the energy increased to –304.0 kcal/mol (a barrier of 42.9 kcal/mol). The peptide bond has extended significantly, to 1.49 Å. From this point on, the energy decreases and the Glu–peptide bond is developing, the energy of the intermediate (INT-1) being –311.2 kcal/mol.

For the protonation of the nitrogen, the $H_1$ proton of water was moved in steps from the water oxygen to the peptide nitrogen. The water molecule was not restricted and only the proton distance to the acceptor nitrogen was monitored. The proton distance from the peptide nitrogen ($H_1$–$N_1$) was reduced from 3.20 to 1.01 Å in steps of 0.01 Å. During this proton transfer, the peptide bond length extended from 1.54 (INT-1) to 1.61 Å (TS-2). The energy barrier for this proton transfer is high, 32.4 kcal/mol (from INT-1 with –311.2 to TS-2 with –278.8 kcal/mol). Following proton transfer, there is a spontaneous extension of the peptide bond, with no energy barrier. In this process, the anhydride is formed with an energy level that is some 20.0 kcal/mol lower than TS-2 (from TS-2 with –278.8 to INT-2 with –298.8 kcal/mol).

The next step in the reaction sequence is the hydrolysis of the anhydride. As a result of proton transfer from water to the peptide, the hydroxide is already "prepared" for the attack on the carbonyl. The hydroxide was moved toward the $C_2$ atom of the anhydride bond, with the $O_1$–$C_2$ distance being reduced from 3.68 to 1.44 Å in steps of 0.01 Å. In the initial structure (INT-2) the distance between the oxygen of hydroxide and the carbon of the carbonyl bond is 3.68 Å and the energy is –298.8 kcal/mol. As the hydroxide moves towards the $C_2$ atom the energy augments until TS-3, in which the distance between the oxygen of hydroxide and the carbon of the carbonyl bond is 2.11 Å and the energy is –286.3 kcal/mol. From this point the energy decreases until the distance between $O_1$–$C_2$ is 1.44 Å (INT-3), and the energy decreases to –316.6 kcal/mol. The energy barrier for this part of the reaction coordinate is thus low, 12.5 kcal/mol.

In the final step, the anhydride bond is broken. It has been extended from 1.47 to 4.00 Å. In the initial structure of this step (INT-3) the bond length between the oxygen of Glu270 and the carbon of the carbonyl bond is 1.47 Å and the energy is –316.6 kcal/mol. As the substrate moves away from Glu270 the energy increases until TS-4, in which the distance between the oxygen of Glu270 and the carbon of the carbonyl bond is 2.0 Å and the energy is –310.2 kcal/mol. From this point the energy decreases and the anhydride bond is broken (3.9 Å), the final energy being stabilized at –359.3

kcal/mol. The energy barrier for this part of the reaction coordinate is thus 6.4 kcal/mol.

## DISCUSSION

We presented three "gas-phase" pathways in order to compare them to previously calculated similar pathways in an "enzyme environment". For studying the alternative pathways of carboxypeptidase A, we employed a semiempirical QM method that has been specifically parametrized to enable calculations of systems that include zinc as well as having multiple H-bonds, MNDO/d/H. Our calculations started from our own X-ray crystallographic results for a CPA complex with a substrate derived inhibitor, which required minimal transformation from crystallography to "create" a substrate.

Out of the three alternatives that were examined, two reaction pathways are of the GAGB type. The third is a direct nucleophilic attack by the enzyme. This last option was recently supported by X-ray studies of a Gly-Tyr complex with CPA [20], where no water molecule was found in the active site and thus, in the absence of water, Gly-Tyr must take the anhydride path. However, Gly-Tyr was found to be bound to CPA in a mode which is significantly different than other peptide substrate analogues. In the crystal structure, this slow substrate uniquely chelates the zinc ion with its peptide carbonyl (which is expected) together with its amino N-terminal group (most probably in the neutral, deprotonated form). The lack of a water molecule in the complex could thus be a special and non-representative case. It is however possible that Gly-Tyr binds to CPA in an "abnormal" mode due to its relatively smaller size compared with longer peptide substrates, explaining also its slow hydrolysis by the enzyme. The binding mode of Gly-Tyr which involves water expulsion from the active site should be nevertheless interesting since most other substrates are much larger and should expel a water molecule even more easily than this smaller substrate.

The direct nucleophilic mechanism is well known in other protease families[49,50]. In serine proteases, the first catalytic step is the acylation of the catalytic serine by the C-terminal of the cleaved peptide. The mechanism of cysteine proteases is basically similar. The direct nucleophilic mechanism was also suggested for aspartic proteases[51] but recent kinetic and X-ray experiments[52] point in the direction of a GAGB mechanism in which a water molecule is critically involved ("push-pull" mechanism)[53].

Our previous computations of three reaction pathways for CPA were done in the presence of a representative region of the active site. The barri-

ers for the two alternative GAGB pathways were found to be around 25 kcal/mol (27.7 kcal/mol for GAGB-1 and 23.4 kcal/mol for GAGB-2, see Figs 4 and 6) relative to the previous step in each of these pathways, while the barrier for the direct nucleophilic attack was much higher, close to 50 kcal/mol (Fig. 8). Is that large value enough for ruling out the direct nucleophilic mechanism? And if it is, are there other arguments to support one of the two GAGB mechanisms?

Reduction of the energy barrier for a reaction is the essence of enzyme catalysis. Such a reduction is defined with respect to another reaction, which does not contain the catalytic machinery. In our computations, we hope to find that part of the reaction which presents a high barrier in the "non-catalytic" environment – while it is substantially lowered in the enzyme environment. Such a comparison may be performed by following the reaction path in the catalytic site of CPA, and comparing it to the same site but without zinc and its close environment, such as the neighboring arginines. For comparing the non-catalytic alternatives we need only the substrate model, a water molecule and a model of Glu270.

At best, the reaction should be compared in a water environment. Major obstacles to such a comparison are: (i) an enormous amount of calculations should is required due to the many closely related structural arrangements of the water molecules and (ii) the direct nucleophilic path which leads to an anhydride is not realistic in a water environment. Therefore, we decided to study the three pathways in the "gas phase", with only the three ingredients: substrate, a single water molecule and Glu270. Gas-phase calculations in comparison to the same pathways in the enzyme environments are summarized graphically in Figs 4, 6 and 8 for GAGB-1, GAGB-2 and the "anhydride" mechanism, respectively. The changes in calculated enthalpies for all three pathways are presented in Table II, starting from a common "zero energy" at the reactants. From the figures, it is clear that the "gas-phase" energy pattern appears to be quite similar to that of the "enzyme environment" which includes the catalytic center and other adjacent residues. In all alternative pathways, the gas-phase curves (red) are higher in energy than the "enzyme environment" all along. However, there is a difference between the GAGB pathways and the nucleophilic pathway ("ANHYD" in Table II). In the GAGB pathways, transition state energies are relatively higher in the gas phase than in the enzyme environment in both TS-1 (36.0 *vs* 14.1 for GAGB-1, 37.4 *vs* 3.2 in GAGB-2) and TS-2 (35.3 *vs* 27.7 in GAGB-1, 30.7 *vs* 23.4 in GAGB-2, see Figs 3 and 5 for the relevant structures), while for the anhydride reaction, TS-2 (32.4 in the gas phase while 48.2 in the enzyme environment) and TS-4 (6.4 *vs* 28.7) are relatively lower

(with respect to the local energy state) in the gas phase than in the enzyme environment.

The energy gain in the pathway from transition states to intermediate species of all reactions (Table II, INT-1, INT-2 energies *etc.*) cannot be fully utilized for surmounting the next energy barrier along the path, as some of each of these energies will be transformed to other vibrations and rotations rather than those of the next transition state modes. Thus, we cannot assume that the relative energies depicted in Table II are meaningful for determining the kinetics of the reaction. To be on the safe side, the barriers in each of the reactions should be assigned to the highest energy peaks, and not to the relatively largest changes along the pathway. Thus, in all reactions, it is TS-2 that is highest in energy, for both gas phase and enzyme environment. This TS is the one for proton transfer to the nitrogen by a proton donor which is different in all three reactions. It is Glu270 in GAGB-1, the substrate C-terminal in GAGB-2 and a water molecule in the "anhydride" mechanism. This proton transfer step promotes the final peptide cleavage in all three reactions. To reach TS-2 from the reactants in the gas phase, the total energy is 51.2 (GAGB-1), 41.7 (GAGB-2) and 68 kcal/mol (ANHYD). The same energy differences in the enzyme environment are 16 (GAGB-1), 12.3 (GAGB-2) and 51.7 kcal/mol (ANHYD). From these energies it is quite clear that the anhydride mechanism is much higher in energy than the GAGB mechanisms in both gas phase and enzyme environment, and the enzyme environment is not substantially different than the gas phase for that mechanism.

TABLE II

Relative energies (in kcal/mol) for consecutive reaction steps in the three pathways, for gas phase and enzyme environment

| Species[a] | TS-1 | INT-1 | TS-2 | INT-2 | TS-3 | INT-3 | TS-4 | Products[b] |
|---|---|---|---|---|---|---|---|---|
| GAGB-1, GP | 36.0 | –20.1 | 35.3 | | | | | –55.6 (–4.4) |
| GAGB-1, EZ | 14.1 | –25.8 | 27.7 | | | | | –65.0 (–49.0) |
| GAGB-2, GP | 37.4 | –26.4 | 30.7 | | | | | –39.9 (1.8) |
| GAGB-2, EZ | 3.2 | –14.3 | 23.4 | | | | | –45.5 (–32.7) |
| ANHYD, GP | 42.9 | –7.3 | 32.4 | –19.9 | 12.5 | –30.3 | 6.4 | –49.0 (–12.3) |
| ANHYD, EZ | 18.6 | –15.1 | 48.2 | –16.4 | 8.3 | –45.0 | 28.7 | –61.7 (–34.4) |

[a] GP, gas phase; EZ, enzyme environment. [b] Values in parenthesis are for the overall enthalpy difference between products and reactants.

The energies to TS-2 of the GAGB mechanisms differ quite similarly between the gas phase and enzyme environment (16/51.2 in GAGB-1, 12.3/41.7 in GAGB-2). The gas-phase energies are much too large for any appreciable reaction to take place without a catalyst. However, the enzyme catalytic site reduces these energies very effectively and both of them are "allowed" by the energy criteria. The decision which of the two is preferred cannot be clearly determined by our methodology, because such small differences of 3–4 kcal/mol may be neutralized by other effects that have not been included, such as entropy differences.

Thus, comparing the gas-phase energies to those in the "enzyme environment" does not change the conclusions reached previously. It is most probable that the anhdyride mechanism does not play any role in peptide cleavage by CPA. It is quite clear that GAGB is the correct mechanism, but we cannot fully support one of the two alternatives for a GAGB pathway, and it is not inconceivable to suggest that a mixture of both could take place under appropriate conditions.

The finding that proton transfer to nitrogen is the rate determining step in the reaction of CPA with a peptide substrate was quite unexpected. In most of the previous studies, the attack by a water molecule on the peptide was suggested to be the rate determining step, in which a high-energy covalent bond is formed while the "resonance" character of the amide is destroyed. In both GAGB pathways, the attack by water has a low transition state, although it is much higher in GAGB-1 (14.1 kcal/mol) than in GAGB-2 (3.2 kcal/mol).

The method of computational reaction mechanisms has always been based on a search for the "lowest-energy path". For a pathway, this consists of searching for the "bottleneck" of a reaction. In comparing pathways, the assignment of the "correct" path is based on lower barriers in one path vis-a-vis the other. Higher barriers in one pathway "prove" that it is not a feasible one. This is a reasonable approach, provided that the path has been adequately modeled, *i.e.*, that the model representation of the reaction pathways is such that the energetics of different pathways might not be reversed by a change of the model. Thus, the model stability is an important issue for its reliability. In enzyme environments, typical changes of models are achieved by increasing the number of residues in the model such that more distant residues are included. This might require very many computations. The "adequacy" of a model cannot be easily resolved and we will not claim that the model presented in this work and in the previous one is ideal. However, we did test the stability of our "small" enzyme environment model (with some 120 atoms) to results of a larger model with nearly

500 atoms, and found some small differences for protonation states in the two[35]. Considering such non-ideal models, no one could argue that a small difference in energy, of the order of a few kcal/mol for the barrier height, allows to make definite declarations about the preference of a pathway in the full enzyme, immersed in its solution environment.

When comparing different pathways for the same reaction, it is clear that the free energy differences between reactants and products should be exactly the same, and it is expected that only the activation energies and those of the intermediates will vary. This is not the case in our computations; in Table II, the last column presents (in parenthesis) the differences in enthalpy of the products from reactants, for gas-phase and enzyme models. Similarity is expected especially in quite similar reactions such as the GAGB mechanisms. GAGB-1 has an overall difference (enzyme environment) between products and reactants of –49 kcal/mol while GAGB-2 has only –33 kcal/mol. Structure changes between the pathways could be one of the sources for such differences: a water molecule that has been removed from the vicinity of zinc to the peptide C-terminal should be less prone to polarization and to attack the carbonyl, thus potentially switching the mechanism from one type of nucleophilic attack by water (GAGB-1) to another type. Having the same water molecule on the "other side" of the substrate, near its C-terminal, could enhance the alternative mechanism (GAGB-2). These movements of a water molecule could possibly be accompanied by fluctuations in the side chain and backbone structure. Such fluctuations exist in protein structures around the "native" or the "complexed" states[54] and display enthalpy differences. Our computations do not follow the full reaction pathway from separated reactants to separated products, which should give a strictly similar difference from products to reactants. We assume a starting position for the reactants which is different in each of the three pathways that were studied.

Could a different proton transfer, by some other protein constituent, present a better option than the ones tested in our reaction pathways? In principle, proton transfer could occur through another water molecule, or, in the case that no such molecule is available in the substrate vicinity, proton transfer could be achieved from one of the protonated arginines – Arg145 or Arg127. This is highly unlikely, as both are bases that would loose a proton much less "willingly" than water.

Another source of error could be the charge state of the system chosen for the simulation. There are not too many choices for this state and there is no easy protocol to determine, computationally, what the protonation state is. It is possible to have started with a protonated Glu270, but the initial at-

tack of Glu270 on the carbonyl would be unfavorable due to the smaller negative charge of the oxygen and the need to transfer the acidic proton prior to attack. There is no possibility to change the charge of the zinc and of its coordinating residues. Also, there is no reason to assume that one of the arginines in this system is not protonated.

Thus, we conclude that, by our gas-phase computations, we may reach a similar conclusion to the one obtained from much larger models: the anhydride pathway is not a viable candidate to be the mechanism of cleavage of peptides by CPA. We have discussed some possible aspects of this reaction pathway, in order to reach this conclusion. However, it is still to be determined whether this pathway could be operating in the case of CPA interacting with other molecules, such as ester substrates. The gas-phase reactions could not help to distinguish between the two GAGB pathways, thus again not adding new knowledge to what has been learnt from the larger models, but at least repeating it, which adds somewhat to the reliability.

The use of MNDO/H/d poses some limit to the ability for calculating proton transfers. Both the original[45] and our own revised[46] versions of MNDO/H dealt with "static H-bonds", and it was shown that at distances larger than *ca* 2.6 Å between proton donor and acceptor, proton transfers could cause discontinuities in the energy of transfer. However, this could be remedied either by comparing similar distances for the transfer when comparing different reactions, by comparing similar transfers (proton from an oxygen to a nitrogen) as well as by a more rigorous approach[55] which was not employed in this study due to the need for transforming a commercial code[47]. In the present study, we compare only similar transfers and we monitored carefully the energy variations upon proton transfers, so that no discontinuities were encountered.

To study the catalytic effect of the active site, it would be best to be able to run reference reactions in solution for all the three pathways. Unfortunately these comparisons are extremely complicated due to the need to position a large number of water molecules and to include their dynamics along any reaction coordinate. QM/MM computations may add more insight into this reaction pathway, and we hope to conduct such computations soon.

*A. Goldblum thanks the Alex Grass Center for Drug Design and Synthesis for partial support of this project.*

**REFERENCES**


1. Vallee B. L., Galdes A.: *Adv. Enzymol. Relat. Areas Mol. Biol.* **1984**, *56*, 283.
2. a) Soffer R. L.: *Annu. Rev. Biochem.* **1976**, *45*, 73; b) Ondetti M. A., Cushman D. W.: *Annu. Rev. Biochem.* **1982**, *51*, 283.
3. a) Malfroy B., Swerts J. P., Guyon A., Roques B. P., Schwartz J. C.: *Nature* **1978**, *276*, 523; b) Schwartz J. C., Gros C., Lecomte J. M., Bralet J.: *Life Sci.* **1990**, *47*, 1279.
4. Hemminges F. J., Farhan M., Rowland J., Banken L., Jain R.: *Rheumatology* **2001**, *40*, 537.
5. Duffy M. J., Maguire T. M., Hill A., McDermott E., O'Higgins N.: *Breast Cancer Res.* **2000**, *2*, 252.
6. Patchett A. A., Cordes E. H.: *Adv. Enzymol. Relat. Areas Mol. Biol.* **1985**, *57*, 1.
7. Vendrell J., Querol E., Aviles F. X.: *Biochim. Biophys. Acta* **2000**, *1477*, 284.
8. Rees D. C., Lewis M., Lipscomb W. N.: *J. Mol. Biol.* **1983**, *168*, 367.
9. Greenblatt H. M., Feinberg H., Tucker P. A., Shoham G.: *Acta Crystallogr., Sect. D: Biol. Crystallogr.* **1998**, *54*, 289.
10. Teplyakov A., Wilson K. S., Orioli P., Mangani S.: *Acta Crystallogr., Sect. D: Biol. Crystallogr.* **1993**, 49, 534.
11. Matthews B. W.: *Acc. Chem. Res.* **1988**, *21*, 333.
12. Lipscomb W. N.: *Proc. Natl. Acad. Sci. U.S.A.* **1980**, 77.
13. Christianson D. W., Lipscomb W. N.: *Acc. Chem. Res.* **1989**, *22*, 62.
14. Vallee B. L., Auld D. S.: *Acc. Chem. Res.* **1993**, *26*, 543.
15. a) Makinen M. W., Kuo L. C., Dymowski J. J., Jaffer S. L.: *J. Biol. Chem.* **1979**, *254*, 356; b) Kuo L. C., Makinen M. W.: *J. Am. Chem. Soc.* **1985**, *107*, 5255; c) Britt B. M., Peticolas W. L.: *J. Am. Chem. Soc.* **1992**, *114*, 5295.
16. Suh J., Park T. H., Hwang B. K.: *J. Am. Chem. Soc.* **1992**, *114*, 5141.
17. Sander M. E., Witzel H.: *Biochem. Biophys. Res. Commun.* **1985**, *132*, 681.
18. Mustafi D., Makinen M. W.: *J. Biol. Chem.* **1994**, *269*, 4587.
19. Lee H. C., Ko Y. H., Baek S. B., Kim D. H.: *Bioorg. Med. Chem. Lett.* **1998**, *8*, 3379.
20. Christianson D. W., Lipscomb W. N.: *Proc. Natl. Acad. Sci. U.S.A.* **1986**, *83*, 7568.
21. Breslow R., Wernick D. L.: *Proc. Natl. Acad. Sci. U.S.A.* **1977**, *74*, 1303.
22. Breslow R., Wernick D. L.: *J. Am. Chem. Soc.* **1976**, *98*, 259.
23. Auld D. S., Galdes A., Geoghegan K. F., Holmquist B., Martinelli R. A., Vallee B. L.: *Proc. Natl. Acad. Sci. U.S.A.* **1984**, *81*, 5041.
24. Lee M., Kim D. H.: *Bioorg. Med. Chem.* **2000**, *8*, 815.
25. Lee K. J., Kim D. H.: *Bioorg. Med. Chem.* **2000**, *6*, 1613.
26. Christianson D. W., Lipscomb W. N.: *J. Am. Chem. Soc.* **1986**, *108*, 545.
27. Christianson D. W., Lipscomb W. N.: *J. Am. Chem. Soc.* **1988**, *110*, 5560.
28. Shoham G., Christianson D. W., Oren D. A.: *Proc. Natl. Acad. Sci. U.S.A.* **1988**, *85*, 684.
29. Feinberg H., Greenblatt H. M., Shoham G. J.: *Chem. Inf. Comp. Sci.* **1993**, *33*, 501.
30. Mock L. W., Zhang J. Z.: *J. Biol. Chem.* **1991**, *266*, 6369.
31. Nakagawa S., Umeyama H., Kitaura K., Morokuma K.: *Chem. Pharm. Bull.* **1981**, *29*, 1.
32. Alex A., Clark T.: *J. Comput. Chem.* **1992**, *13*, 704.
33. a) Alvarez-Santos S., Gonzalez-Lafont A., Lluch J. M., Oliva B., Aviles F. X.: *Can. J. Chem.* **1994**, *72*, 2077; b) Alvarez-Santos S., Gonzalez-Lafont A., Lluch J. M., Oliva B., Aviles F. X.: *New J. Chem.* **1998**, *22*, 319.

34. Abashkin Y. G., Burt S. K., Collins J. R., Cachau R. E., Russo R. N., Erickson J. W. in: *Metal–Ligand Interactions* (N. Russo and D. R. Salahub, Eds), Vol. 474, p. 1. Kluwer, Dordrecht 1996.
35. Kilshtain-Vardi A., Goldblum A., Shoham G.: *Int. J. Quantum Chem.* **2002**, *88*, 87.
36. Banci L., Bertini I., La Penna G.: *Proteins* **1994**, *18*, 186.
37. Kilshtain-Vardi A., Goldblum A., Shoham G.: *J. Mol. Phys.* **2002**, submitted.
38. Feinberg H., Greenblatt H. M., Behar V., Gilon S., Cohen S., Bino A., Shoham G.: *Acta. Crystallogr., Sect. D: Biol. Crystallogr.* **1995**, *51*, 428.
39. Kilshtain-Vardi A., Shoham G.: Unpublished results.
40. a) Ewenson A., Cohen-Suissa R., Levian-Teitelbaum D., Selinger Z., Chorev M., Gilon C.: *Int. J. Pept. Protein Res.* **1988**, *31*, 269; b) Ewenson A., Laufer R., Chorev M., Selinger Z., Gilon C.: *J. Med. Chem.* **1988**, *31*, 416.
41. Seroussi D., Glick M., Goldblum A.: Unpublished results.
42. Giessner-Prettre C., Jacob O.: *J. Comput.-Aided Mol. Des.* **1989**, *3*, 23.
43. Thiel W., Voityuk A. A.: *Theor. Chim. Acta* **1992**, *81*, 391.
44. Brauer M., Kunert M., Dinjus E., Klussman M., Doring M., Gorls H., Anders E.: *J. Mol. Struct.* **2000**, *505*, 289.
45. Burstein K. Ya., Isaev A. N.: *Theor. Chim. Acta* **1984**, *64*, 397.
46. Goldblum A.: *J. Comput. Chem.* **1987**, *6*, 835.
47. Oxford Molecular Inc.: UNICHEM 5.0, 1999.
48. Flanigan M. C., Komornicki A., McIver J. W. in: *Semiempirical Methods of Electronic Structure Calculations, Part B: Applications* (G. A. Segal, Ed.), p. 1. Plenum Press, New York and London 1977.
49. Polgar L.: *Biol. Chem. Hoppe–Seyler* **1990**, *371*, Suppl. 327.
50. Polgar L., Halasz P.: *Biochem. J.* **1982**, *207*, 1.
51. Fruton J. S. in: *Enzymes* (P. D. Boyer, Ed.), 3rd ed., Vol. 3, p. 119. Academic Press, New York 1971.
52. a) Antonov V. K., Ginodman L. M., Rumsh L. D., Kapitannikov Yu. V., Barshevskaya T. N., Yavashev L. P., Gurova A. G., Volkova L. I.: *Eur. J. Biochem.* **1982**, *117*, 195; b) James M. N. G., Sielecki A. R.: *Biochemistry* **1985**, *24*, 3701.
53. Polgar L.: *FEBS Lett.* **1987**, *219(1)*, 1.
54. Shortle D., Simons K. T., Baker D.: *Proc. Natl. Acad. Sci. U.S.A.* **1998**, *95*, 11158.
55. Goldblum A.: *J. Mol. Struct. (THEOCHEM)* **1988**, *179*, 153.